Continuous monitoring of electromyography (EMG), mechanomyography (MMG), sonomyography (SMG) and torque output during ramp and step isometric contractions

Jing-Yi Guo[1], Yong-Ping Zheng[1, 2*], Hong-Bo Xie[1, 3], Xin Chen[1]

[1]Department of Health Technology and Informatics,

[2]Research Institute of Innovative Products and Technologies, The Hong Kong Polytechnic University, Hong Kong, China

[3]Department of Biomedical Engineering, Jiangsu University, Zhenjiang, China

[*]Corresponding author:

Dr. Yong-Ping Zheng

Address: Department of Health Technology and Informatics,
Research Institute of Innovative Products and Technologies,
The Hong Kong Polytechnic University,
Hung Hom, Kowloon, Hong Kong SAR, China

Tel: +852 27667664

Fax: +852 23624365

Email: ypzheng@ieee.org (Dr Yong-Ping Zheng)
ejingyiguo@hotmail.com (Ms Jing-Yi Guo)

Submitted to:

Medical Engineering & Physics

First submission: Jan 28 2010

Abstract

In this study we simultaneously collected ultrasound images, EMG, MMG from the rectus femoris (RF) muscle and torque signal from the leg extensor muscle group of nine male subjects (mean±SD, age = 30.7±.4.9 years; body weight = 67.0±8.4 kg; height = 170.4±6.9 cm) during step, ramp increasing, and decreasing at three different rates (50%, 25% and 17% MVC/s). The muscle architectural parameters extracted from ultrasound imaging, which reflect muscle contractions, were defined as sonomyography (SMG) in this study. The cross-sectional area (CSA) and aspect ratio between muscle width and thickness (width/thickness) were extracted from ultrasound images. The results showed that the CSA of RF muscles decreased by 7.25±4.07% when muscle torque output changed from 0% to 90% MVC, and the aspect ratio decreased by 41.66±7.96%. The muscle contraction level and SMG data were strongly correlated (R^2=0.961, P=0.003, for CSA and R^2=0.999, P<0.001, for width/thickness ratio). The data indicated a significant differences (P<0.05) in percentage changes for CSA and aspect ratio among step, ramp increasing, and decreasing contractions. The normalized EMG RMS in ramp increasing was 8.25±4.00% higher than step (P=0.002). The normalized MMG RMS of step contraction was significantly lower than ramp increasing and decreasing, with averaged differences of 12.22±3.37% (P=0.001) and 12.06±3.37% (P=0.001), respectively. The results of this study demonstrated that the CSA and aspect ratio, i.e., SMG signals, can provide useful information about muscle contractions. They may therefore complement EMG and MMG for studying muscle activation strategies under different conditions.

Index Terms- **Muscle; Soft Tissue; Ultrasound; Sonomyography; SMG; Mechanomyography; MMG; Electromyography; EMG.**

1. Introduction

Electromyography (EMG) is generated by a record of the electrical discharges of active motor units (MU) during the muscle activation [1], and the root mean square (RMS) magnitude of EMG is commonly used to describe the time-domain information of the EMG signal [2]. As the "mechanical counterpart" of the motor unit electrical activity measured by EMG, mechanomyography (MMG) is a recording of mechanical oscillation that is detected from the body surface overlying the muscle [3, 4]. It has been suggested that the lateral oscillations detected by MMG can be decomposed into three parts: (1) a gross lateral movement at the beginning of a muscle contraction, (2) smaller subsequent lateral oscillations produced at the resonant frequency of the muscle, and (3) dimensional changes of the muscle fiber [4, 5].

As the index of torque during muscle contraction [5, 6], EMG and MMG signals can each provide information on various aspects of muscle function. For example, EMG has now been widely used to study muscle fatigue [7, 8], muscle pathology [9-12], prosthetic device control [13, 14], etc. The features of the MMG signal have been used to reflect the kinematic and physiological characteristics of postural control [15], concentric muscle contractions [16], and cycle ergometry [17,18], as well as to detect various muscular disorders, including cerebral palsy [19], myotonic dystrophy [20], low back pain [21], and muscle fatigue [22]. Furthermore, studies have been conducted with EMG and MMG simultaneously to examine skeletal muscle characteristics. For example, EMG and MMG were used to compare agonist vs. antagonist muscles in old vs. young women [6] and to estimate the influence of torque changes during relaxation from maximal voluntary contraction (MVC) of elbow flexors at different joint angles [23]. Additionally, complementary knowledge was provided by collecting EMG and MMG during concentric, isometric and eccentric contractions at different MVC [24]. These modalities were also used to investigate the effect of acute static stretching on the biceps brachii [23] and to assess lower-back muscle fatigue [21].

Recently, many studies have been performed using EMG and MMG to identify the motor control strategies involved in force/torque production during isometric ramp increasing or step contraction, in which the force/torque is alternately linearly increased or steadily maintained [25]. Investigating the differences between various muscle contraction protocols may guide exercise testing and training [26]. The amplitude and frequency of MMG and EMG were examined with torque during ramp increasing or step contraction [4, 27-30]. For example, EMG has been used to illustrate the different characteristics of ramp increasing vs. step contractions [31-34], and the relationship between MMG and force/torque has also been compared [35].

On the other hand, ultrasonography has been effectively employed to evaluate the morphological changes in muscle thickness or displacement [36-40], muscle fiber, pennation angle [44, 45], and cross-sectional area [46, 47]. It has also been suggested that ultrasound parameters may characterize muscular pain, injury and dysfunction [48-52]. Moreover, ultrasonography has been used along with EMG to provide more comprehensive information about the activities and properties of skeletal muscles [53-57]. We have recently proposed using the real-time muscle morphological change detected by ultrasound, namely sonomyography (SMG), for the prosthetic control [58,59] and for assessment of isometric muscle contraction [60-62] and isotonic contraction [63,64].

According to the literature, EMG and MMG have been used as indicators to compare different motor control strategies in ramp increasing vs. step contractions [25,26,29,31,32,35]. Yet the utility of the architectural changes detected by ultrasound for evaluation of the difference between these contractions has not been comprehensively investigated. Since data suggest that the motor control strategy may differ between ramp increasing and step contractions [25,26,29,31,32,35], it is possible that different motor control strategies may be recruited during step, ramp increasing and decreasing, in which torque is produced to a greater or lesser degree. Therefore, the purpose of this study was to simultaneously collect and compare EMG, MMG and SMG vs. torque relationships during ramp increasing, decreasing and step contractions and hopefully to investigate the differences in the motor control strategy of ramp and step contractions with respect to morphological characteristics, including muscle cross-sectional area (CSA) and aspect ratio between width and thickness (width/thickness ratio).

2. Methods

2.1. Subjects

Nine healthy male adults (mean±SD, age = 30.7±.4.9 years; body weight = 67.0±8.4 kg; height = 170.4±6.9 cm) volunteered to participate in this study. No participant had a history of neuromuscular disorders, and all were aware of experimental purposes and procedures. Human subject ethical approval was obtained from the relevant committee in the authors' institution, and informed consent was obtained from each subject prior to the experiment.

2.2. Experiment protocol

The subject was seated with the right leg at a flexion angle of 90° below the horizontal plane on a calibrated dynamometer (Humac/Norm Testing and Rehabilitation System, Computer Sports Medicine, Inc., Massachusetts, USA). Straps on the subject's trunk were used to stabilize his position (Fig. 1). The testing position of the subject was in accordance with the Humac/Norm User's Guide (Humac/Norm Testing and Rehabilitation System, Computer Sports Medicine, Inc., Massachusetts, USA. 2006). The subject was required to put forth his maximal effort of isometric knee extension for a period of 3 s with verbal encouragement provided. The maximal voluntary contraction (MVC) was defined as the highest value of torque recorded during the entire isometric contraction [65]. A rest of 5 min was allowed before the subject performed a second MVC test. The MVC torque was then calculated by averaging the two recorded highest torque values from the two tests.

The subject was instructed to perform step, ramp increasing, and decreasing contractions, the order of which was chosen randomly. For the step contraction, the subject was required to produce a stable sub-maximal MVC torque (15, 30, 45, 60, 75, and 90% MVC) respectively for 4 s. During the ramp increasing and decreasing, each subject was instructed to produce torques increasing from 0 to 90% of his MVC, decreasing back to zero linearly within 4, 8, and 12 s, during which the corresponding contraction rates were 50% MVC/s, 25% MVC/s, and 17% MVC/s, respectively. The reason for choosing 90% MVC as the highest value was to avoid muscle fatigue. During each contraction, a template and the real-time torque values were shown on a computer screen. The former served as a target, and these two lines helped subjects to adjust their torque productions in real time. Each test was repeated twice with a rest of 5 min between two adjacent trials. Before the actual test, subjects practiced producing a smooth ramp contraction for several times. The ramp contractions with tracking error (TE) smaller than 3% MVC [28] were selected for subsequent data processing. The tracking error was defined as follows:

$$T = \sqrt{\frac{1}{N-1}\sum_{n=1}^{N}(Torque(n) - Template(n))^2} \tag{1}$$

where *Torque (n)* is the actual torque recorded during each test, *Template (n)* is the pre-designed linear pattern shown on a computer screen to guide the ramp contraction, and N is the number of torque signal data points recorded during each test.

2.3. Data Acquisition

The isometric torque generated by the right quadriceps femoris muscle was measured using a Norm dynamometer (Humac/Norm Testing and Rehabilitation System, Computer Sports Medicine, Inc., Massachusetts, USA) and sampled at a frequency of 25 Hz, which was the frame rate of B-mode ultrasound imaging. A commercial ultrasound scanner (Ultrasound Diagnostic Scanner, EUB-8500, Hitachi Medical Corporation, Tokyo, Japan) with a 12 MHz linear array ultrasound probe (L53L, Hitachi Medical Corporation, Tokyo, Japan) was used to collect the ultrasound images. The long axis of the ultrasound probe was arranged perpendicularly to the long axis of the thigh on its superior aspect, three-fifths of the distance from the anterior superior iliac spine to the superior patellar border [66, 67]. The ultrasound probe was fixed by a multi-degree custom-designed adjustable bracket. Ultrasound gel was applied between the skin and probe to serve as an acoustic coupling medium (Fig. 1). The probe was adjusted to optimally visualize the muscle fiber [56] and the position was marked to ensure that the probe was placed at the same site every time. Before the test began, the ultrasound images were collected for the subject under the relaxed state for normalization of the parameters collected during the contraction tests. The B-mode ultrasound images were displayed in real time and digitized by a video card (NI PCI-1411, National Instruments, Austin, USA) at 25 Hz for later analysis.

Two surface EMG electrodes were placed on the rectus femoris (RF) muscle belly parallel with the long axis of the muscle, and the ultrasound probe was positioned between them. It has been earlier reported that the ultrasound gel used during the test generates negligible effects to the EMG recording [68]. An MMG sensor was placed close to one of the EMG electrodes, which was at a shorter distance from the knee than the other electrode (Fig. 1). The surface EMG signal was captured by the EMG bipolar Ag-AgCl electrodes (Axon System, Inc., NY, USA), and a reference EMG electrode was placed near the kneecap. The MMG signal was detected using an accelerometer (EGAS-FS-10-/V05, Measurement Specialties, Inc., France) fixed with two-sided tape. The surface EMG and MMG signals were amplified by a custom-designed amplifier with a gain of 2000, filtered separately by 10-400 Hz, 5-100Hz band-pass analog filters within the amplifier, and digitized by a 12-bit data acquisition card (NI-DAQ 6024E, National Instruments Corporation, Austin, TX, USA) with a sampling rate of 1 KHz. Ultrasound images, surface EMG, MMG and torque signals were simultaneously collected and stored by software for ultrasonic measurement of motion and elasticity (UMME, http://www.tups.org) for further analysis. The time delay between the different data collection systems was calibrated using a method similar to that described by Huang et al. [68]. As the transducer moved cyclically up and down in a water tank, the two signals representing the ultrasound image and the simulated EMG, respectively, were collected and stored. The time delay between the data sets was calculated using a cross-correlation algorithm. The details can be found in our earlier study [68].

2.4. Data Analysis

All signals were processed off-line using a program written in Matlab (Version 7.3, MathWorks, Inc., Massachusetts, USA). During each sub-maximal step contraction, a 1-s epoch of data was selected from the middle of the 4-s muscle contraction duration. The torque value was represented by the mean of the data within the 1-s epoch (Fig. 2). For ramp contraction, 256-ms epochs of data were selected from the centre of the torque to match the value in step contraction (Fig. 3). The mean torque, and root mean square (RMS) values of EMG and MMG were calculated for each epoch, and the EMG/MMG RMSs were expressed as a percentage of their maximal values at 90% MVC. B-mode ultrasound images were synchronized with the torque signal. In other words, a given B-mode ultrasound image frame corresponded to a given torque value point. The B-mode ultrasound images corresponding to torque values that were close to the averaged torque value calculated during step contraction were selected for ramp increasing, decreasing and step contractions. The width, thickness and cross-sectional area (CSA) of the RF muscle were measured from the ultrasound images [69] using ImageJ software (ImageJ, National Institutes of Health, USA) as shown in Fig. 4. In addition to CSA, the width/thickness ratio of the RF muscle was used to describe the morphological change during contractions (Fig. 5). The ultrasound parameters were then normalized as the percentage change, with the reference value taken while the subject was relaxed in the same position.

A total of 294 (6×6×2 (step) ＋6×6×3×2 (ramp) + 6×1 (relaxed state)) ultrasound images were measured twice by the same investigator. The intra-class correlation (ICC) based on one-way random model and standard error of the measurement (SEM) were performed to evaluate intra-observer repeatability. The relationships for CSA, width/thickness ratio, EMG and MMG RMS vs. % MVC were investigated by a power model for the averaged value across the nine subjects and three types of isometric contractions (step, ramp increasing, and decreasing). Four separate three-way repeated measure analyses of variance (ANOVAs) (movement patterns [step vs. ramp increasing vs. decreasing] × % MVC [15% vs. 30% vs. 45% vs. 60% vs. 75% vs. 90%]×velocity [50% MVC/s vs. 25% MVC/s vs. 17% MVC/s]) were used to analyze normalized EMG/MMG RMS, CSA, and width/thickness ratio, respectively. If there were no significant interaction effect among these three factors, two- and one-way repeated measures ANOVAs were followed up with Bonferroni pairwise comparisons [35]. The relationships between CSA, width/thickness ratio, MMG RMS, EMG RMS versus %MVC were examined for each individual and the mean values for all the subjects. Polynomial regression analysis (linear, quadratic, and cubic) were used to examine the relationships. All the data were analyzed using SPSS (SPSS Inc. Chicago, IL, USA).

Statistical significance was set at the 5% probability level.

3. Results

3.1 Composite (mean) of ultrasound measurements of the RF muscle during step and ramp increasing, decreasing contractions

The ICC for width, thickness and CSA measurements of RF muscle in this study were 0.986, 0.987, and 0.978 respectively, and the SEM were 0.13 cm, 0.04 cm and 0.48 cm² (Table 1). The overall values of CSA and width/thickness ratio from the nine subjects' RF muscles were 9.83±3.06 cm² (mean ± SD) and 2.99±0.57, respectively, during the relaxed state. As shown in Fig. 6, the relationships between both the percentage change of CSA and width/thickness ratio vs. % MVC could be well represented by cubic functions (R^2 =0.961, P=0.003, for CSA and R^2 =0.999, P<0.001, for width/thickness ratio).

There were no significant three- or two-way interactions among the three factors (movement patterns×% MVC×velocity, all P>0.05), but the effects of the movement patterns (P<0.001) and % MVC (P=0.012) on the CSA were significant. The percentage change at 15% MVC was found to be significantly lower than at 75% MVC (reduced by 2.94±0.93%, P=0.026) or 90% MVC (reduced by 3.21±0.93%, P=0.010). The percentage change of CSA during step was significantly lower than during ramp decreasing, with mean difference of 2.75±0.82% (P=0.003). While the corresponding reduction compared with ramp increasing was 0.64±0.82%, no significant difference was demonstrated (p>0.999). In addition, the percentage change of CSA during ramp increasing was 2.11±0.58% lower than during ramp decreasing with significant effect (P=0.001) (Fig. 7).

For the width/thickness ratio, there were no significant three-way or two-way interactions for movement patterns×velocity and movement patterns×% MVC, but there was a significant effect for two-way interactions for movement patterns×% MVC ($P=0.002$). As shown in Fig. 8, we noted that the change of width/thickness ratio in ramp decreasing was 5.42±1.65% and 6.93±1.17% higher than in both step and ramp increasing, respectively ($P=0.003$ and $P<0.001$), and the difference between step and ramp increasing was not significant ($P>0.999$).

3.2 Composite (mean) of the EMG and MMG RMS of RF muscle during step, ramp increasing, and decreasing contractions

As shown in Fig. 9, the overall relationships of both the normalized EMG RMS and MMG RMS vs. % MVC were well represented by cubic models with high R^2 values ($R^2 = 0.999$, $P<0.001$, for EMG RMS and $R^2 = 0.999$, $P<0.001$, for MMG RMS). Movement patterns and % MVC were each found to significantly affect the EMG RMS (both $P<0.001$). It was demonstrated that the normalized EMG RMS was increased as the increase of torque (all $P<0.05$). The normalized EMG RMS in ramp increasing was 8.25±4.00% higher than step ($P=0.002$) ($P<0.001$). Although the average normalized EMG RMS of ramp decreasing was 4.25±2.38% higher than, step contraction and 4.00±1.68% lower than ramp increasing, no significant difference was demonstrated ($P=0.225$ and 0.054) (Fig. 10).

The normalized MMG RMS of step contraction was significantly lower than ramp increasing and decreasing, with averaged differences of 12.22±3.37% ($P=0.001$) and 12.06±3.37% ($P=0.001$), respectively. The difference between ramp increasing and decreasing was small and not obvious (0.16±2.38%, Fig. 11). Significant effects of velocity and % MVC for normalized MMG RMS were found (both P<0.01). MMG RMS was only found to be significantly higher at a velocity of 50% MVC/s than at 17% MVC/s (P<0.001). Moreover, the averaged MMG RMS became significantly higher as % MVC increased (all P<0.05), with the exception of the change from 15% to 30% MVC, and 30% MVC to 45% MVC (P>0.999) (Fig. 9).

3.3 Inter-individual variability of polynomial regression analysis of CSA, width/thickness ratio, EMG RMS, MMG RMS

Table 1 shows the polynomial regression analyses for the individual CSA, width/thickness ratio, EMG RMS, MMG RMS versus isometric torque relationships. For the individual patterns of CSA, five of the nine subjects exhibited cubic, three exhibited a quadratic; for width/thickness ratio, five best fit with cubic, two with quadratic and one with linear regression. For EMG and MMG RMS, there are still five subjects exhibit cubic. However, three exhibit quadratic for EMG RMS whereas only one exhibit quadratic and linear for MMG RMS.

4. Discussion

In this paper, ultrasound images, EMG, MMG and torque signals were continuously collected from the RF muscles of nine male subjects during step, ramp increasing, and decreasing contractions at rates of 50, 25 and 17% MVC/s. The CSA and width/thickness ratio were extracted from the ultrasound images to describe the architectural changes of the RF muscle during isometric contractions. The intra-operator reliability for ultrasound measurements of RF muscle in this study was excellent, ranging from 0.978 to 0.987 (Table 1). This reliability in ultrasound measurement was achieved by careful control of the transducer's position and orientation. Studies have shown that muscle functions, such as the amplitude of force produced, joint angle change, muscle contraction pattern (step or ramp) are closely related to architectural characteristics such as CSA [65-71] and thickness [36,60, 63,64,72-74]. The CSA of RF muscle of the younger male participants in this study (9.83 ± 3.06 cm^2) was similar to those observed in [71] using magnetic resonance imaging. In another study using ultrasonography, the reported CSA of RF muscle was 4.6 ± 1.33 cm^2 for the older male subjects [66]. The CSA of RF muscle reported was smaller mainly because the subjects recruited were much older (around 60 years old) than that used in current study. It has been suggested that reduction in muscle CSA develops during the aging process due to a decrease in motor units [75].

During the isometric contractions, the CSA of the RF muscle was measured by directly tracing the position of the aponeurosis, which separates the RF muscle from the neighboring muscles of the quadriceps femoris (Fig. 4). The results showed that the CSA decreased more as torque increased, with an average percentage change from $6.61 \pm 9.03\%$ (15% MVC) to $10.27 \pm 8.77\%$ (90% MVC) (Fig. 6A). On the other hand, the percentage change of width/thickness ratio indicated that as torque increased, the width of the RF muscle diminished, while the thickness increased (Fig. 6B). During the development of quadriceps femoris' torque output, the RF muscle is often regarded as the bi-articular muscle that transfers moments between joints [76] and directs force and movement [77], while the other three vasti are synergistic, mono-articular muscles that generate force [78-79]. Ploutz-Snyder et al. suggested that the RF muscle was the inactive muscle, based on their findings of no change in CSA after squat exercises [71]. In contrast, in the present study, although the CSA of the RF muscle decreased with increasing torques, the results of the width/thickness ratio suggested that the RF muscle was actively involved in isometric torque development, as indicated by its increasing thickness and decreasing width. These observations strongly support the concept that the RF muscle is likely to act as a mono-articular body [79]. However, to support this conclusion, future studies are warranted.

The morphological differences in the RF muscle in step, ramp increasing, and decreasing may suggest different activation strategies in each of these three isometric contractions. Movement patterns significantly affect the CSA and width/thickness ratio ($P<0.05$). Both the CSA and width/thickness ratio of RF muscle were significantly higher in step compared with ramp decreasing, and the width/thickness ratio of ramp increasing was significantly higher than of ramp decreasing at all velocities ($P<0.05$). Akima et al. suggested that not all muscle fibers are recruited, even at the MVC, for subjects with low physical training [80]; furthermore, according to the muscle size principle, motor units are recruited in the order of their recruitment thresholds [81]. As muscle torque developed, the CSA and width/thickness ratio of RF muscle decreased. Thus, the smaller values seen in ramp increasing compared with step may indicate that more muscle motor units were recruited and that more fast-twitch muscle fibers may have been activated for ramp increasing than for step. The motor units of fast-twitch were controlled by the large size of motor neuron, which was recruited at higher thresholds [82]. Therefore, the increased ratio between the recruited motor unit of fast-twitch and slow-twitch in ramp increasing might allow subjects to gradually increase torque; this mechanism may require extra effort to recruit high-threshold motor units. Ramp decreasing occurs in a reverse process compared to ramp increasing. However, the CSA and width/thickness ratio of RF muscle in ramp decreasing was deduced by a comparison to ramp increasing (Fig. 7 and 8). As the torque was linearly reduced, the deformation of the RF muscle in ramp decreasing could not restore muscle function to the same level as in ramp increasing, possibly due to viscoelasticity of the skeletal muscle and surrounding media. Another reason may be that the effort needed to produce the same level of torque in the torque-increasing process was lower than for torque-decreasing, which was used to recruit high-threshold motor units. Other reasons too may affect muscle behavior during different movement patterns, such as the actin-myosin cross-bridge activity, intramuscular pressure, muscle stiffness, the mechanical properties of neighboring tissues [24], and the ratio of fast-twitch and slow-twitch fibers [83]. Since the ratio of the fibre type could vary greatly in different types of muscle [84], the current SMG parameters should be tested on other skeletal muscles for a solid conclusion. The findings of a curvilinear increase in EMG and MMG amplitude vs. torque were consistent with those reported in previous studies [29, 85]. EMG and MMG RMS increased progressively with increasing torque at all velocities, suggesting that more muscle motor units were recruited as torque developed.

Both EMG and MMG amplitude in the RF muscle were found to be smaller in step contraction than in ramp increasing, which was consistent with results from the plantar flexors in studies performed by Bilodeau et al. [86] and Ryan et al. [28]. However, in a departure from previous studies examining the EMG and MMG performance in step vs. ramp increasing contractions [25,32,35,87-88], the present study also investigated the EMG and MMG amplitude in ramp decreasing contractions in order to comprehensively compare all of the movement protocols that may be used in muscle training or rehabilitation. We found that the EMG RMS of ramp decreasing contractions was significantly smaller than that of ramp increasing and bigger than that of the step test. However, the difference between ramp increasing and decreasing was not significant in the MMG RMS. The contraction rate did have a significant effect on the MMG RMS, perhaps because MMG signals are easily contaminated by noise during muscle contractions [89]. At higher rates, the low-frequency movement at the beginning or end of isometric contractions would affect the MMG signals. This may also explain the large increase in MMG RMS at 60% MVC of ramp decreasing contractions at a rate of 50% MVC/s (Fig. 11A). Our results are in line with findings from previous studies that have indicated that the isometric contraction patterns ramp increasing, ramp decreasing and step may each require motor control strategies that differ in, for example, the relative contributions of motor unit recruitment and firing rate modulation [31,35,83].

Moreover, the differences among ramp increasing, decreasing and step contractions were observed in the electrophysiological (EMG), mechanical (MMG), morphological (SMG) responses. SMG parameters at most percentages of MVC increased from ramp decreasing to ramp increasing to step, while EMG and MMG RMS parameters increased from step to ramp decreasing to ramp increasing. We noticed a discrepancy between the SMG parameters and EMG/MMG RMS during ramp increasing and decreasing contraction; this may indicate that the morphological parameter would not always yield the same conclusion as the electrophysiological or mechanical parameter. The mechanisms responsible for this phenomenon should be further investigated, and if this finding can be confirmed by testing more subjects, SMG parameters may provide information complementary to EMG and MMG.

The results of inter-individual variability of polynomial regression analysis indicated that the composite CSA, width/thickness ratio, EMG RMS and MMG RMS versus isometric torque relationship were all best fit with a cubic model. However, only 55.5% (five of nine) exhibited the same cubic patterns as the composite relationship (Table 1). The quadratic relationship was take 33.3%, 22.2%,33.3%, 11.1% for CSA, width/thickness ratio, MMG RMS and EMG RMS. There was only 11.1% exhibit linear for width/thickness ratio and MMG RMS, whereas 11.1% of the individual patterns exhibited no significant relationship for CSA, width/thickness ratio, EMG RMS versus torque and 22.2% for MMG RMS. The EMG, MMG result of the present study was consistent with previous studies suggesting that the surface EMG and MMG amplitude versus isometric torque relationship should be evaluated on a subject-by-subject basis [90, 91] and that there were differences between subjects for the MMG amplitude versus isometric torques [92, 93]. On the other hand, the SMG parameters also showed the inter-individual variability. This may caused by the differences in motor control strategies [94, 95] or muscle fiber type composition [96], which deserves further study.

Based on the sample size of 9 and alpha of 0.05, the calculated mean statistical power for the parameters showed significances between different percentages of MVC is 0.61; that for comparison between ramp increasing and decreasing parameters is 0.65; and that for comparison between ramp and step parameters is 0.71. The overall mean statistical power is 0.66 for all parameters. It is noted that statistical powers of the parameters were relatively small, particularly for SMG and MMG parameters. This result is consistent with the large standard deviations observed for the SMG and MMG parameters. In future studies, more subjects are required and the reasons for the relatively larger variations of SMG and MMG parameters among subjects should be investigated

To sum up, the combination of ultrasonography, EMG and MMG recordings during three isometric contractions revealed the non-linear relationships between SMG (CSA, width/thickness ratio) and torque, EMG and torque, and MMG and torque for the RF muscle. As the utilization of different motor control strategies under various movement patterns has not been comprehensively studied, the present study provides data regarding morphological changes of the RF muscle in different movement patterns (ramp increasing, decreasing, and step) using ultrasound. We found that the different movement patterns significantly affect the CSA and width/thickness ratio; in other words, our ultrasound measurement data of the RF muscle suggested that different movement patterns may use different motor control strategies to control muscle morphology. The EMG/MMG data from this study were consistent with findings from previous studies and support the suggestion that different motor control strategies may be utilized during various movement patterns. The discrepancy between SMG parameters and EMG/MMG RMS regarding to ramp increasing and decreasing contraction should be further studied.

Furthermore, the reasons for the relatively larger variations of SMG parameters among subjects should be investigated in future studies. The recording system described here can be used to obtain more comprehensive information regarding muscle activities by simultaneously recording electrophysiological, mechanical, and morphological responses in human skeletal muscle activity.

Acknowledgements

This work was supported by The Hong Kong Polytechnic University (G-U699, J-BB69) and the Grant Council of Hong Kong (PolyU 5331/06E). We thank Mr. Huang Yanping for his help in obtaining the bracket, as well as all of our subjects for their kind support of this study.

Figure Captions

Fig. 1. Experimental setup for collecting ultrasound images, EMG, MMG and torque signals from the subject's right rectus femoris (RF) muscle during isometric ramp increasing, decreasing and step contractions. The ultrasound probe was aligned perpendicularly to the RF muscle belly using a multi-degree adjustable bracket. The two surface EMG electrodes were located at the two sides of the ultrasound transducer and in parallel with the muscle fibers. The MMG sensor was placed near the EMG electrode.

Fig. 2. A typical example of MMG and EMG signals recorded from RF muscle of subject C during step contraction at the 45% MVC level. The signals (MMG, EMG, torque) between the dashed lines were selected to represent the characteristics of a 45% MVC step.

Fig. 3. A typical example of MMG and EMG signals recorded from the RF muscle of subject C during ramp contractions at the rate of 25% MVC/s. The vertical dashed boxes represent twelve segments of data points analyzed as MVC increased from 15% to 90% and again as MVC decreased from 90% to 15% at 15% intervals.

Fig. 4. (A) The aponeuroses appear as hyperechoic strips and boundaries differentiating RF muscle from other neighboring quadriceps muscles (vastus lateralis (VL), vastus intermedius (VI), and vastus medialis (VM)). The central aponeurosis of the RF muscle appears as a comma-shaped hyperechoic band [69]. (B) The CSA, width and thickness were measured by ImageJ software for further analysis.

Fig. 5. Typical ultrasound images at 0%, 30%, 60%, and 90% MVC contraction levels during ramp contractions at the rate of 17% MVC/s from subject C.

Fig. 6. The relationship between (A) averaged percentage change of cross-sectional area vs. % MVC, and (B) the averaged percentage change of width/thickness ratio vs. % MVC across nine subjects in isometric contraction.

Fig. 7. The percentage change of cross-sectional area at different isometric torque (MVC) during the step and ramp increasing, decreasing contractions with torque changing rates of (A) 50% MVC/s, (B) 25% MVC/s, and (C) 17% MVC/s. Values are mean ± SD (N=9).

Fig. 8. The percentage change of width/thickness ratio at different isometric torque (MVC) during step, ramp increasing, and decreasing contractions with torque at rates of (A) 50% MVC/s, (B) 25% MVC/s, and (C) 17% MVC/s. Values are mean ± SD (N=9).

Fig. 9. Normalized (A) EMG RMS vs. % MVC and (B) MMG RMS vs. % MVC for nine subjects in isometric contraction.

Fig. 10. Normalized EMG RMS during step, ramp increasing, and decreasing contractions with torque at rates of (A) 50% MVC/s, (B) 25% MVC/s, and (C) 17% MVC/s. Values are mean ± SD (N=9).

Fig. 11. Normalized MMG RMS at different isometric torques (MVC) during step, ramp increasing, and decreasing contractions with torque at rates of (A) 50% MVC/s, (B) 25% MVC/s, and (C) 17% MVC/s. Values are mean ± SD (N=9).

Table 1. The intra-class correlation coefficients (ICC) and standard errors of measurement (SEM) for the width, thickness, and cross-sectional area (CSA) of rectus femoris (RF) muscle from two repeated ultrasound measurements made by one operator.

Ultrasound parameter	ICC	95% CI lower	95% CI upper	SEM
Width	0.986	0.985	0.988	0.13 cm
Thickness	0.987	0.986	0.989	0.04 cm
CSA	0.978	0.975	0.981	0.48 cm^2

Table 2. The polynomial regression models for the change of cross-sectional area (CSA), width/thickness ratio, mechanomyography and electromyography root mean square (MMG RMS and EMG RMS) vs. percent maximal voluntary contraction (% MVC) relationship.

Subject	CSA		Width/thickness ratio		EMG RMS		MMG RMS	
	Model	R^2	Model	R^2	Model	R^2	Model	R^2
1	Cubic	0.992	Linear	0.831	Cubic	0.997	Cubic	0.997
2	Cubic	0.999	Cubic	0.987	NS	NS	Cubic	0.986
3	Cubic	0.990	Quadratic	0.998	Quadratic	0.996	Cubic	0.999
4	Quadratic	0.926	Cubic	0.999	Quadratic	0.999	Cubic	0.999
5	Cubic	0.998	Cubic	0.997	Cubic	0.999	Cubic	0.998
6	Cubic	0.999	Cubic	0.994	Cubic	0.999	NS	NS
7	Quadratic	0.942	Quadratic	0.993	Cubic	0.999	Linear	0.723
8	NS	NS	Cubic	0.982	Cubic	0.981	NS	NS
9	Quadratic	0.934	NS	NS	Quadratic	0.986	Quadratic	0.986
Mean	Cubic	0.998	Cubic	0.999	Cubic	0.998	Cubic	0.999

NS: no significant model (P>0.05)

Figures

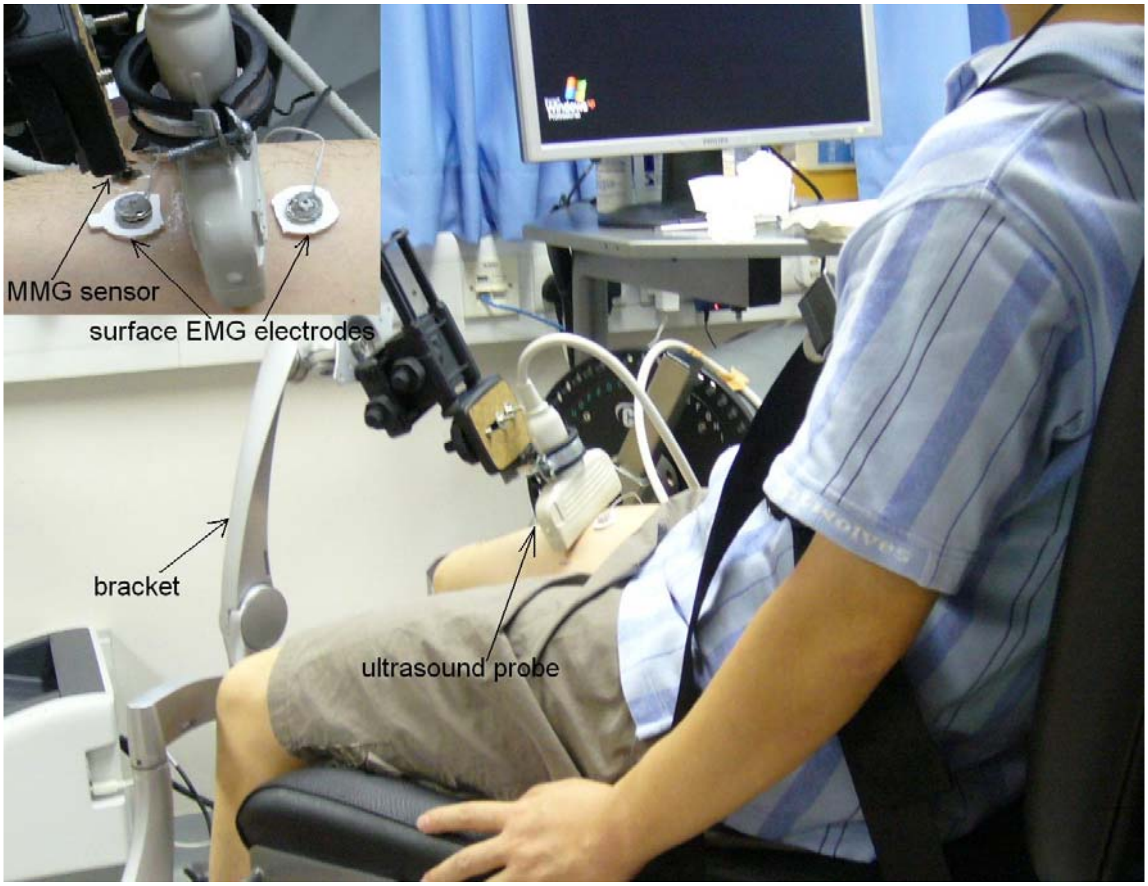

Fig. 1

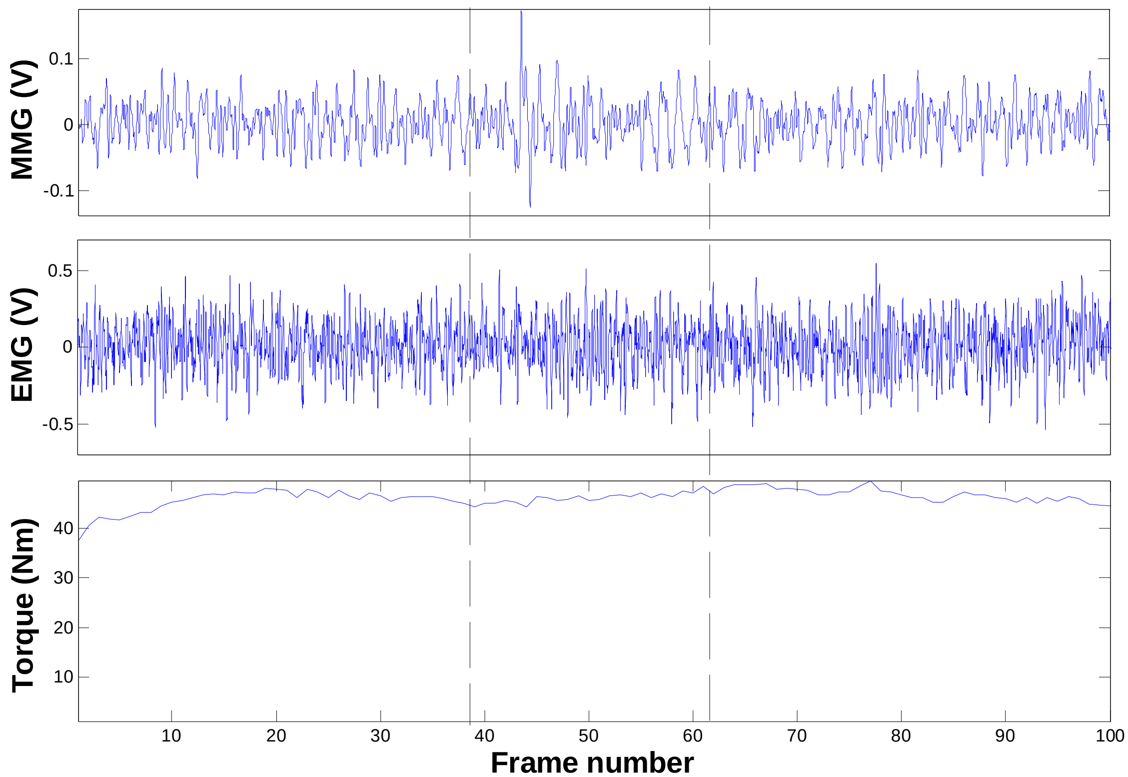
MMG (V)
0.1
0
-0.1
EMG (V)
0.5
0
-0.5
Torque (Nm)
40
30
20
10
10
20
30
40
50
60
70
80
90
100
Frame number

Fig. 2

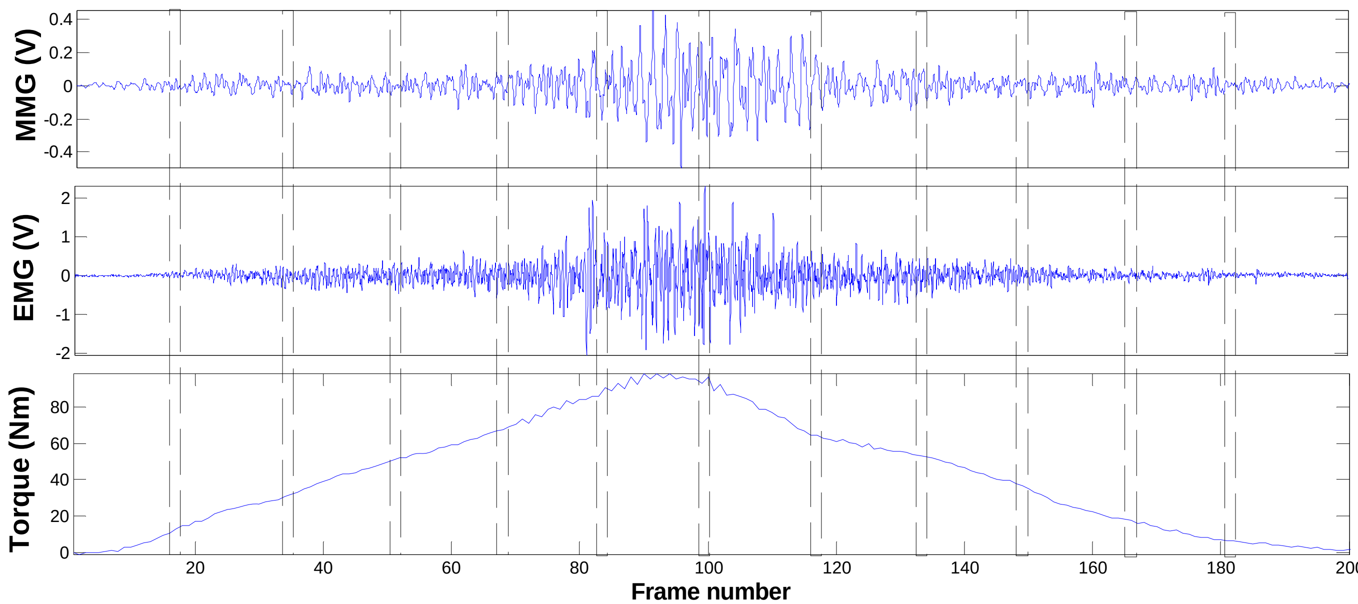
MMG (V)
EMG (V)
Torque (Nm)
Frame number

Fig. 3

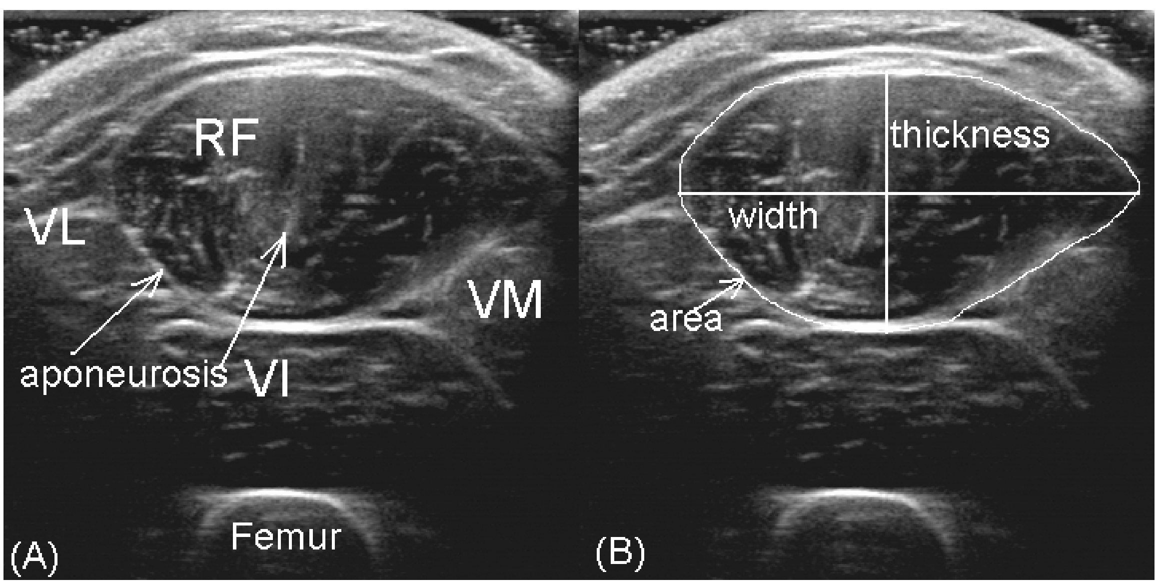
RF
VL
VM
VI
aponeurosis
Femur
(A)
(B)
thickness
width
area

Fig. 4

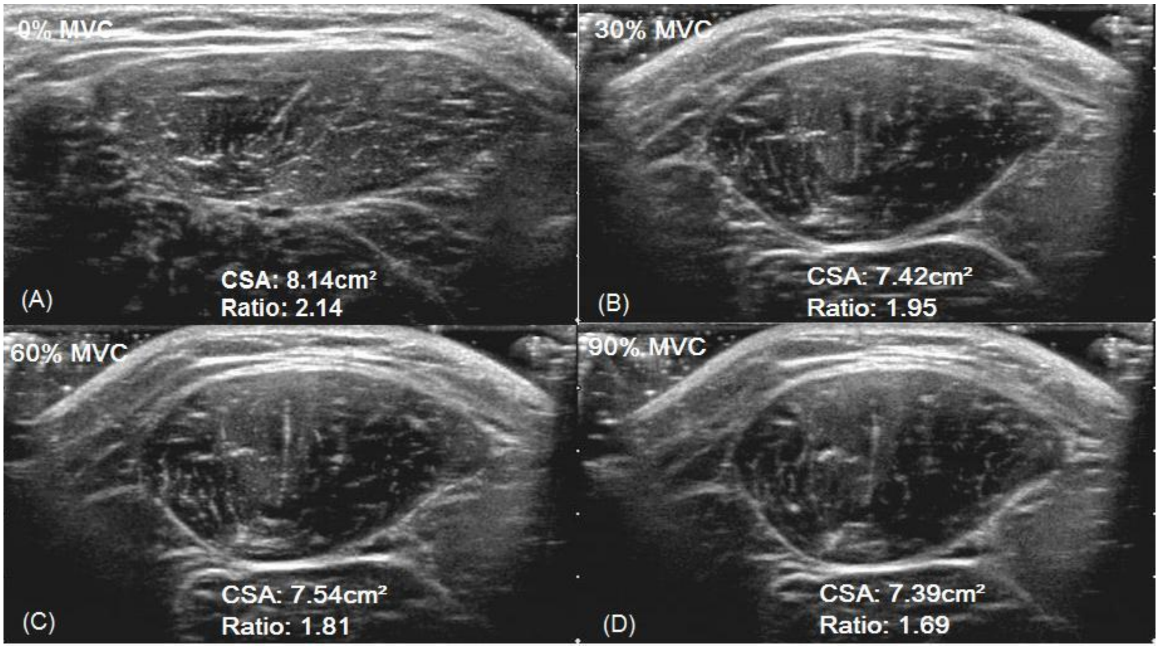
0% MVC
CSA: 8.14cm²
Ratio: 2.14
(A)
30% MVC
CSA: 7.42cm²
Ratio: 1.95
(B)
60% MVC
CSA: 7.54cm²
Ratio: 1.81
(C)
90% MVC
CSA: 7.39cm²
Ratio: 1.69
(D)

Fig. 5

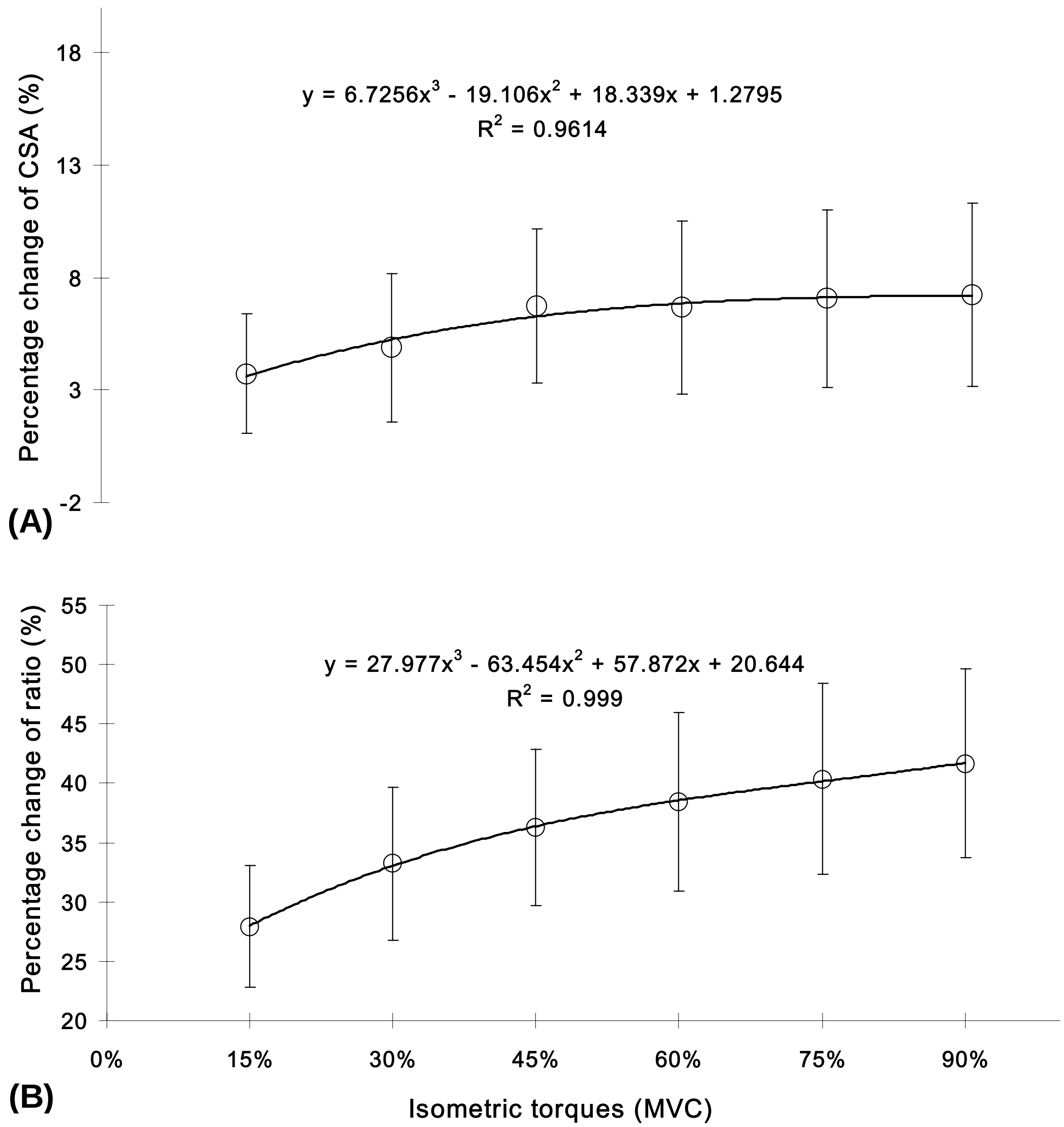
y = 6.7256x3 - 19.106x2 + 18.339x + 1.2795
R2 = 0.9614
Percentage change of CSA (%)
18
13
8
3
-2
(A)
y = 27.977x3 - 63.454x2 + 57.872x + 20.644
R2 = 0.999
Percentage change of ratio (%)
55
50
45
40
35
30
25
20
0%
15%
30%
45%
60%
75%
90%
(B)
Isometric torques (MVC)

Fig.6

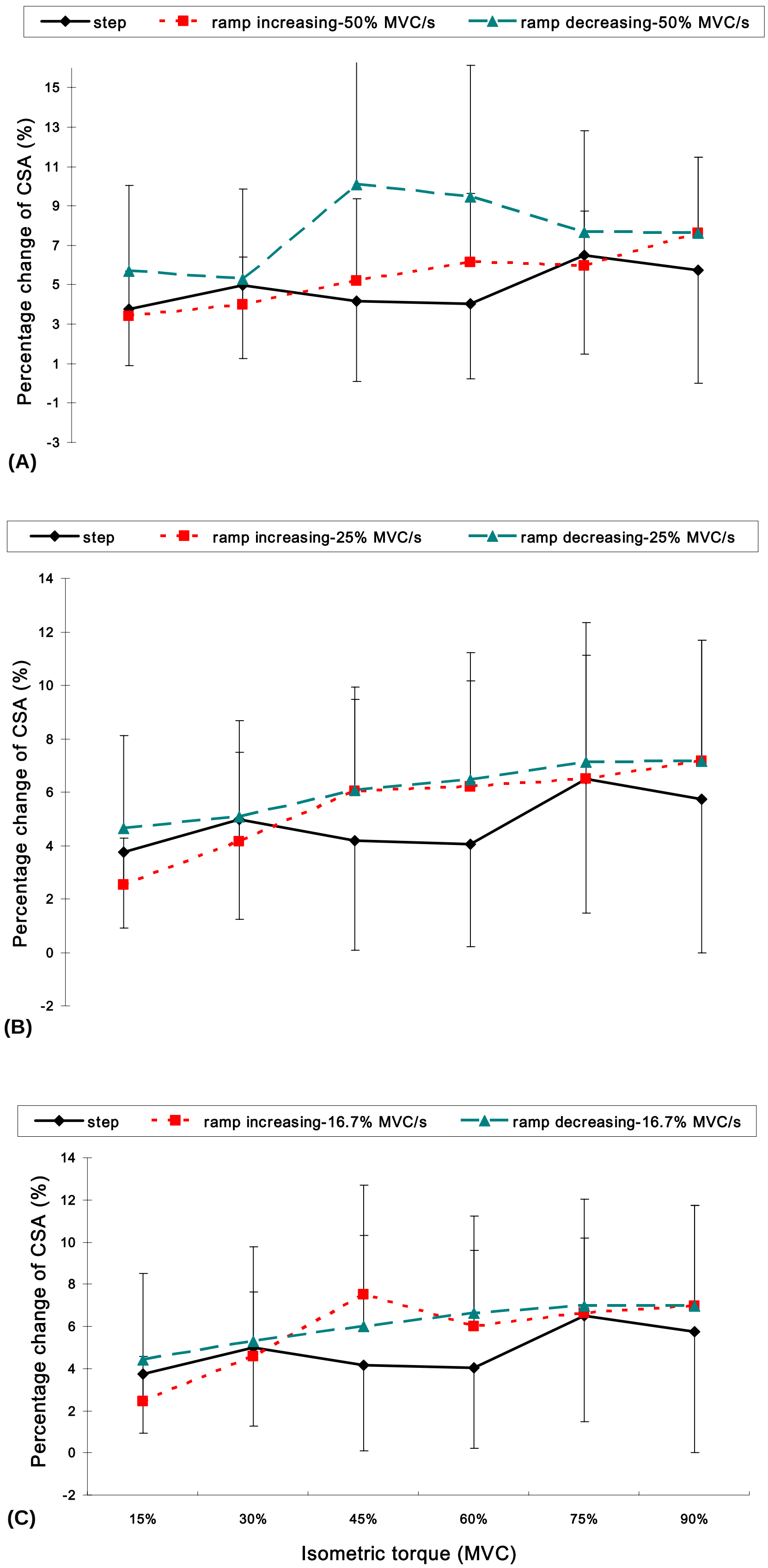
step
ramp increasing-50% MVC/s
ramp decreasing-50% MVC/s
Percentage change of CSA (%)
(A)
step
ramp increasing-25% MVC/s
ramp decreasing-25% MVC/s
Percentage change of CSA (%)
(B)
step
ramp increasing-16.7% MVC/s
ramp decreasing-16.7% MVC/s
Percentage change of CSA (%)
(C)
15%
30%
45%
60%
75%
90%
Isometric torque (MVC)

Fig. 7

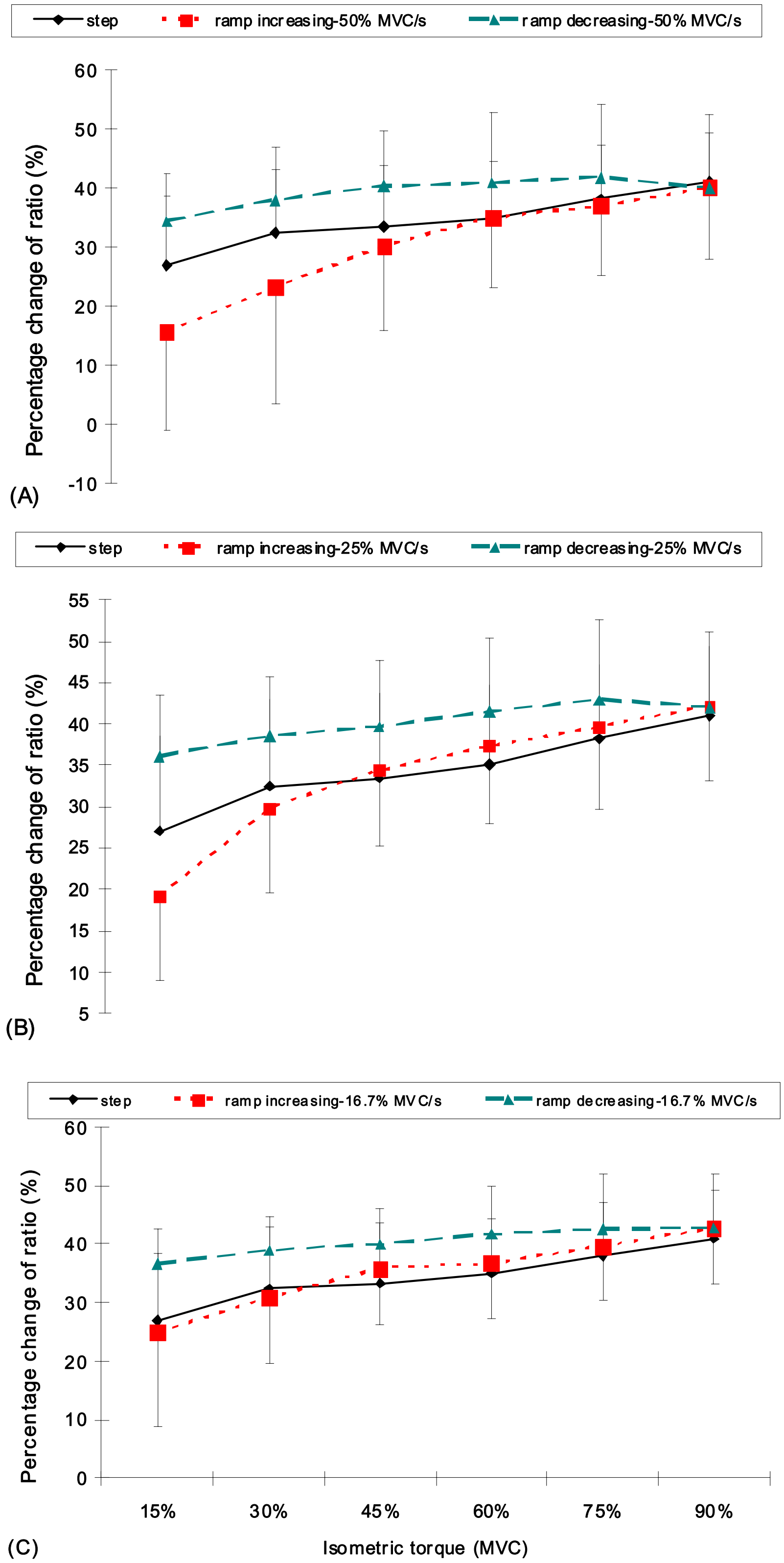
step
ramp increasing-50% MVC/s
ramp decreasing-50% MVC/s
Percentage change of ratio (%)
(A)
step
ramp increasing-25% MVC/s
ramp decreasing-25% MVC/s
Percentage change of ratio (%)
(B)
step
ramp increasing-16.7% MVC/s
ramp decreasing-16.7% MVC/s
Percentage change of ratio (%)
15%
30%
45%
60%
75%
90%
Isometric torque (MVC)
(C)

Fig. 8

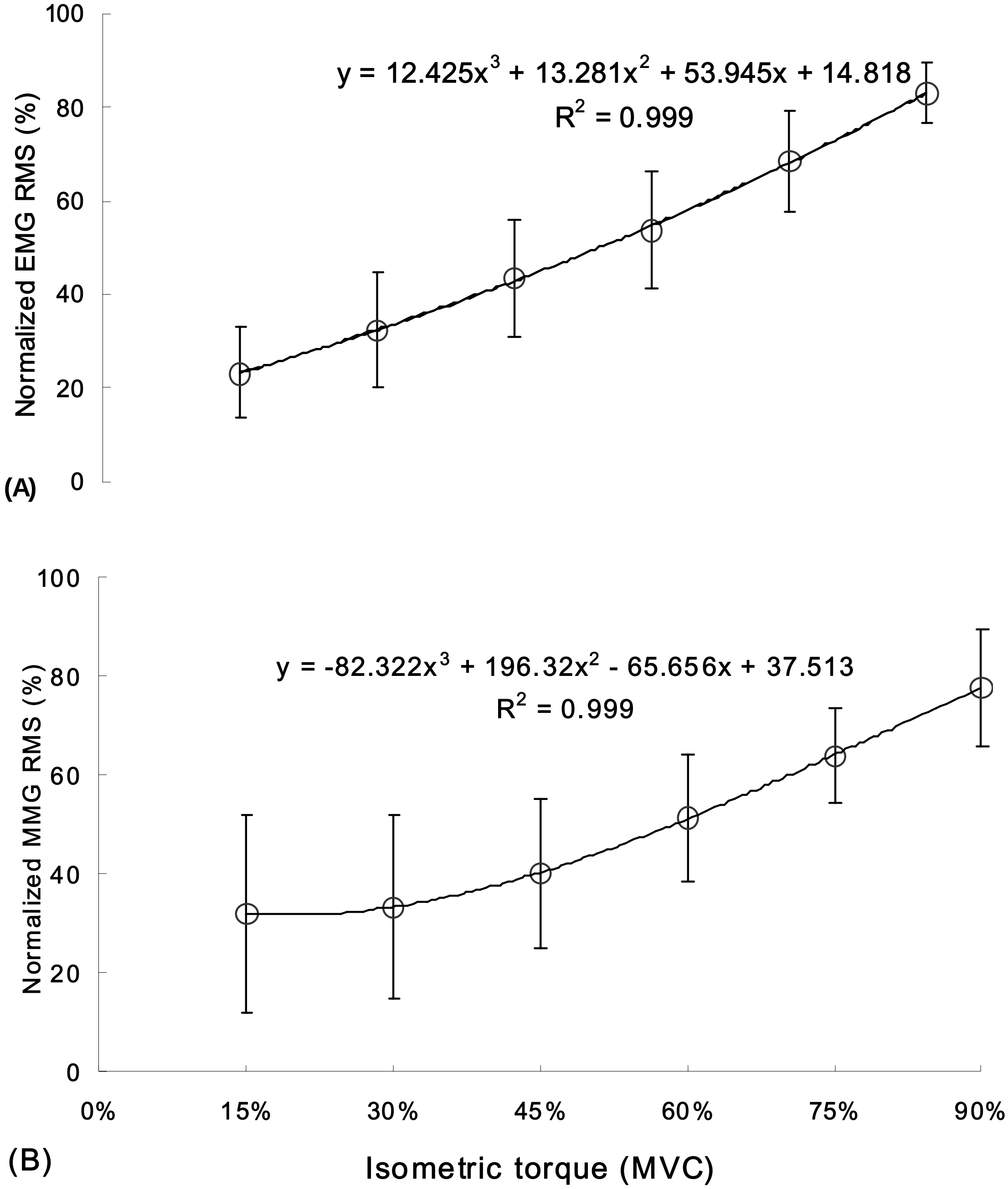
y = 12.425x3 + 13.281x2 + 53.945x + 14.818
R2 = 0.999
Normalized EMG RMS (%)
100
80
60
40
20
0
(A)
y = -82.322x3 + 196.32x2 - 65.656x + 37.513
R2 = 0.999
Normalized MMG RMS (%)
100
80
60
40
20
0
0%
15%
30%
45%
60%
75%
90%
(B)
Isometric torque (MVC)

Fig. 9

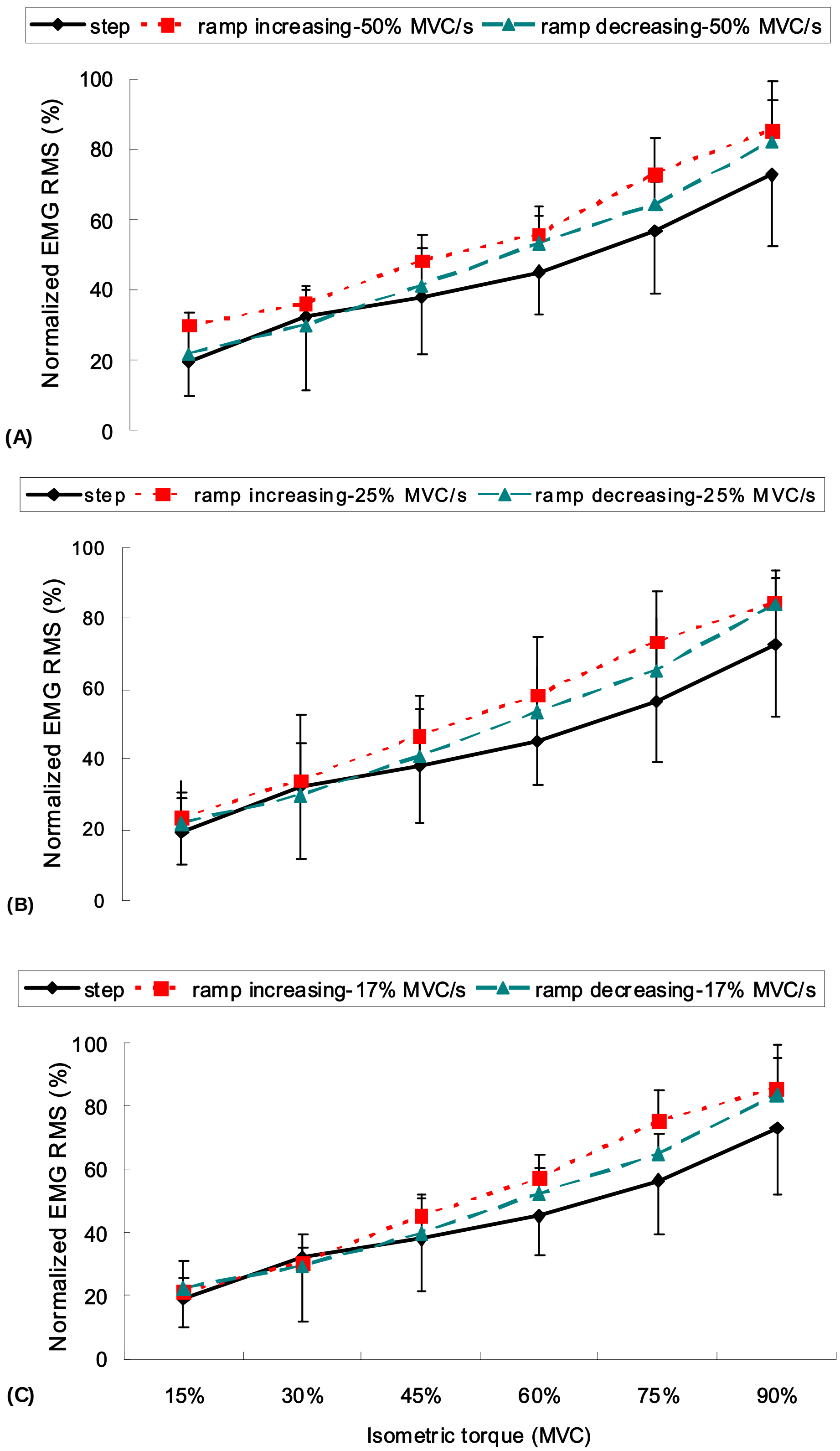
step
ramp increasing-50% MVC/s
ramp decreasing-50% MVC/s
Normalized EMG RMS (%)
(A)
step
ramp increasing-25% MVC/s
ramp decreasing-25% MVC/s
Normalized EMG RMS (%)
(B)
step
ramp increasing-17% MVC/s
ramp decreasing-17% MVC/s
Normalized EMG RMS (%)
(C)
15%
30%
45%
60%
75%
90%
Isometric torque (MVC)

Fig. 10

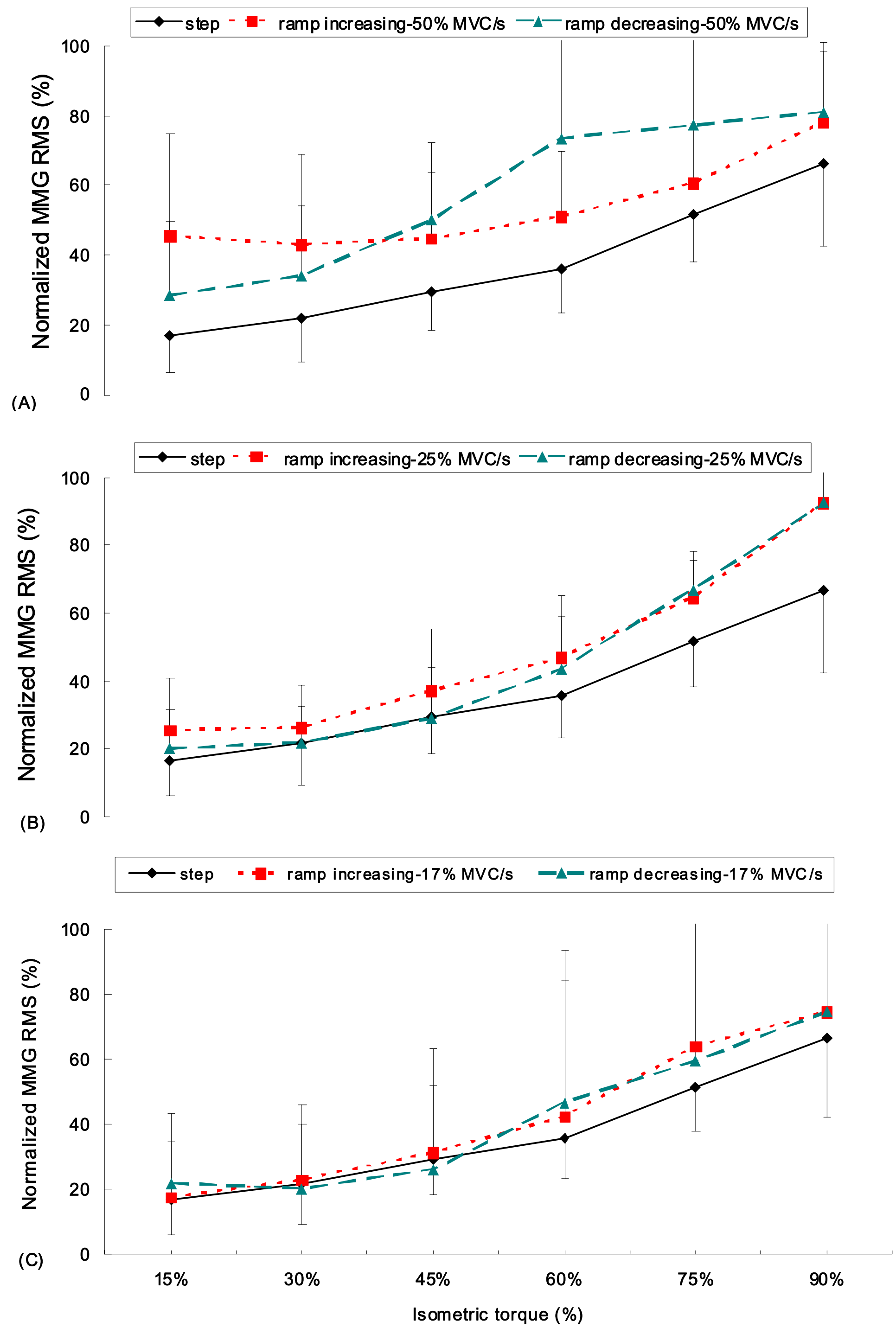
step
ramp increasing-50% MVC/s
ramp decreasing-50% MVC/s
Normalized MMG RMS (%)
(A)
step
ramp increasing-25% MVC/s
ramp decreasing-25% MVC/s
Normalized MMG RMS (%)
(B)
step
ramp increasing-17% MVC/s
ramp decreasing-17% MVC/s
Normalized MMG RMS (%)
(C)
15%
30%
45%
60%
75%
90%
Isometric torque (%)

Fig. 11

References

[1] Zwarts MJ, Stegeman DF. Multichannel surface EMG: Basic aspects and clinical utility. Muscle Nerve 2003; 28:1-17.

[2] Karlsson S，Gerdle B. Mean frequency and signal amplitude of the surface EMG of the quadriceps muscles increase with increasing torque - a study using the continuous wavelet transform. J Electromyogr Kines 2001; 11:131-40.

[3] Gordon G, Holbourn AH. The sounds from single motor units in a contracting muscle. J Physiol 1948; 107:456-64.

[4] Beck TW, Housh TJ, Johnson GO, Weir JP, Cramer JT, Coburn JW, Malek MH. Mechanomyographic amplitude and mean power frequency versus torque relationships during isokinetic and isometric muscle actions of the biceps brachii. J Electromyogr Kinesiol 2004; 14:555-64.

[5] Orizio C. Muscle sound: bases for the introduction of a mechanomyographic signal in muscle studies. Crit Rev Biomed Eng 1993; 21:201-43.

[6] Jaskolska A, Kisiel-Sajewicz K, Brzenczek-Owczarzak W, Yue GH, Jaskolski A. EMG and MMG of agonist and antagonist muscles as a function of age and joint angle. J Electromyogr Kines 2006; 16:89-102.

[7] Masuda K, Masuda T, Sadoyama T, Inaki M, Katsuta S. Changes in surface EMG parameters during static and dynamic fatiguing contractions. J Electromyogr Kinesiol 1999; 9:39-46.

[8] Fukuda K, Umezu Y, Shiba N, Tajima F, Nagata K. Electromyographic fatigue analysis of back muscles during remote muscle contraction. J Back Musculoskelet 2006; 19:61-6.

[9] Haig AJ, Gelblum JB, Rechtien JJ, Gitter AJ. Technology assessment: The use of surface EMG in the diagnosis and treatment of nerve and muscle disorders. Muscle Nerve 1996; 19:392-5.

[10] Hogrel JY. Clinical applications of surface electromyography in neuromuscular disorders. Neurophysiol Clin 2005; 35:59-71.

[11] Labarre-Vila A. Assessment of muscle function in pathology with surface electrode EMG. Rev Neurol-France 2006; 162:459-65.

[12] Ohata K, Tsuboyama T, Ichihashi N, Minami S. Measurement of muscle thickness as quantitative muscle evaluation for adults with severe cerebral palsy. Phys Ther 2006; 86:1231-9.

[13] Boostani R, Moradi MH. Evaluation of the forearm EMG signal features for the control of a prosthetic hand. Physiol Meas 2003; 24:309-19.

[14] Soares A, Andrade A, Lamounier E ,Carrijo R. The development of a virtual Myoelectric prosthesis controlled by an EMG pattern recognition system based on neural networks. J Intell Inf Syst 2003; 21:127-41.

[15] Kouzaki M, Fukunaga T. Frequency features of mechanomyographic signals of human soleus muscle during quiet standing. J Neurosci Meth 2008; 173:241-8.

[16] Ebersole KT, Housh TJ, Johnson GO, Evetovich TK, Smith DB, Perry SR. MMG and EMG responses of the superficial quadriceps femoris muscles. J Electromyogr Kinesiol 1999; 9: 219-27.

[17] Housh TJ, Perry SR, Bull AJ, Johnson GO, Ebersole KT, Housh DJ, deVries HA. Mechanomyographic and electromyographic responses during submaximal cycle

ergometry. Eur J Appl Physiol 2000; 83:381-7.
[18] Perry SR, Housh TJ, Weir JP, Johnson GO, Bull AJ, Ebersole KT. Mean power frequency and amplitude of the mechanomyographic and electromyographic signals during incremental cycle ergometry. J Electromyogr Kinesiol 2001; 11:299-305.
[19] Akataki K, Mita K, Itoh K, Suzuki N, Watakabe M. Acoustic and electrical activities during voluntary isometric contraction of biceps brachii muscles in patients with spastic cerebral palsy. Muscle Nerve 1996; 19:1252-7.
[20] Orizio C, Esposito F, Sansone V, Parrinello G, Meola G, Veicsteinas A. Muscle surface mechanical and electrical activities in myotonic dystrophy. Electromyogr Clin Neurophysiol 1997; 37:231-9.
[21] Yoshitake Y, Ue H, Miyazaki M, Moritani T. Assessment of lower-back muscle fatigue using electromyography, mechanomyography, and near-infrared spectroscopy. Eur J Appl Physiol 2001; 84:174-9.
[22] Mamaghani NK, Shimomura Y, Iwanaga K, Katsuura T. Mechanomyogram and electromyogram responses of upper limb during sustained isometric fatigue with varying shoulder and elbow postures. J Physiol Anthropol Appl Human Sci 2002; 21:29-43.
[23] Jaskolska A, Kisiel K, Brzenczek W, Jaskolski A. EMG and MMG of synergists and antagonists during relaxation at three joint angles. Eur J Appl Physiol 2003; 90:58-68.
[24] Madeleine P, Bajaj P, Sogaard K, Arendt-Nielsen L. Mechanomyography and electromyography force relationships during concentric, isometric and eccentric contractions. J Electromyogr Kinesiol 2001; 11:113-21.
[25] Bilodeau M, Cincera M, Arsenault AB and Gravel D. Normality and stationarity of EMG signals of elbow flexor muscles during ramp and step isometric contractions. J Electromyogr Kinesiol 1997; 7:87-96.
[26] Bader DS, Maguire TE, Balady GJ. Comparison of ramp versus step protocols for exercise testing in patients > or = 60 years of age. Am J Cardiol 1999; 83: 11-4.
[27] Akataki K, Mita K, Watakabe M, Itoh K. Mechanomyogram and force relationship during voluntary isometric ramp contractions of the biceps brachii muscle. Eur J Appl Physiol 2001; 84:19-25.
[28] Ryan ED, Cramer JT, Egan AD, Hartman MJ, Herda TJ. Time and frequency domain responses of the mechanomyogram and electromyogram during isometric ramp contractions: A comparison of the short-time Fourier and continuous wavelet transforms. J Electromyogr Kinesiol 2008a; 18:54-67.
[29] Akasaka K, Onishi H, Momose K, Ihashi K, Yagi R, Handa Y, Hoshimiya N. EMG power spectrum and integrated EMG of ankle planterflexors during stepwise and ramp contractions. Tohoku J Exp Med 1997; 182:207-16.
[30] Beck TW, Housh TJ, Johnson GO, Weir JP, Cramer JT, Coburn JW, Malek MH. Gender comparisons of mechanomyographic amplitude and mean power frequency versus isometric torque relationships. J Appl Biomech 2005; 21:96-109.
[31] Bilodeau M, Arsenault AB, Gravel D, Bourbonnais D. EMG power spectra of elbow extensors during ramp and step isometric contractions. Eur J Appl Physiol 1991; 63:24-8.

[32] Lariviere C, Arsenault AB, Gravel D, Gagnon D, Loisel P. Effect of step and ramp static contractions on the median frequency of electromyograms of back muscles in humans. Eur J Appl Physiol 2001; 85:552-9.
[33] Nadeau S, Bilodeau M, Delisle A, Chmielewski W, Arsenault AB, Gravel D. The influence of the type of contraction on the masseter muscle EMG power spectrum. J Electromyogr Kinesiol 1993; 3:205-13.
[34] Sanchez JH, Solomonow M, Baratta RV, Dambrosia R. Control Strategies of the Elbow Antagonist Muscle Pair during 2 Types of Increasing Isometric Contractions. J Electromyogr Kinesiol 1993; 3:33-40.
[35] Ryan ED, Beck TW, Herda TJ, Hartman MJ, Stout JR, Housh TJ, Cramer JT. Mechanomyographic amplitude and mean power frequency responses during isometric ramp vs. step muscle actions. J Electromyogr Kinesiol 2008b; 168:293-305.
[36] Nogueira W, Gentil P, Mello SNM, Oliveira RJ, Bezerra AJC, Bottaro M. Effects of power training on muscle thickness of older men. Int J Sports Med 2009; 30:200-4.
[37] Matsubayashi T, Kubo J, Matsuo A, Kobayashi K, Ishii N. Ultrasonographic measurement of tendon displacement caused by active force generation in the poas major muscle. J Physiol Sci 2008; 58:323-32.
[38] Bojsen-Moller J, Hansen P, Aagaard P, Kjaer M， Magnusson SP. Measuring mechanical properties of the vastus lateralis tendon-aponeurosis complex in vivo by ultrasound imaging. Scand J Med Sci Sports 2003; 13:259-65.
[39] Springer BA, Gill NW. Characterization of lateral abdominal muscle thickness in persons with lower extremity amputations. J Orthop Sports Phys Ther 2007; 37:635-43.
[40] Mannion AF, Pulkovski N, Gubler D, Gorelick M, O'Riordan D, Loupas T, Schenk P, Gerber H, Sprott H. Muscle thickness changes during abdominal hollowing: an assessment of between-day measurement error in controls and patients with chronic low back pain. Eur. Spine J. 2008; 17:494-501.
[41] Okita M, Nakano J, Kataoka H, Sakamoto J, Origuchi T, Yoshimura T. Effects of therapeutic ultrasound on joint mobility and collagen fibril arrangement in the endomysium of immobilized rat soleus muscle. Ultrasound Med Biol 2009; 35:237-44.
[42] Ichinose Y, Kawakami Y, Ito M, Fukunaga T. Estimation of active force-length characteristics of human vastus lateralis muscle. Acta anatomica 1997; 159:78-83.
[43] Maganaris CN. Force-length characteristics of in vivo human skeletal muscle. Acta Physiol Scand 2001; 172:279-85.
[44] Kawakami Y, Abe T, Fukunaga T. Muscle-Fiber Pennation Angles Are Greater in Hypertrophied Than in Normal Muscles. J Appl Physiol 1993; 74:2740-4.
[45] Mahlfeld K, Franke J, Awiszus F. Postcontraction changes of muscle architecture in human quadriceps muscle. Muscle Nerve 2004; 29:597-600.
[46] Kanehisa H, Ikegawa S, Tsunoda N, Fukunaga T. Strength and cross-sectional areas of reciprocal muscle groups in the upper arm and thigh during adolescence. Int J Sports Med 1995; 16:54-60.
[47] Narici MV, Binzoni T, Hiltbrand E, Fasel J, Terrier F, Cerretelli P. In vivo human gastrocnemius architecture with changing joint angle at rest and during graded

isometric contraction. J Physiol-London 1996; 496:287-97.

[48] Botteron S, Verdebout CM, Jeannet PY, Kiliaridis S. Orofacial dysfunction in Duchenne muscular dystrophy. Arch Oral Biol 2009; 54:26-31.

[49] Diaz JFJ, Rey GA, Matas RB, De La Rosa FJB, Padilla EL, Vicente JGV. New technologies applied to ultrasound diagnosis of sports injuries. Adv Ther 2008; 25:1315-30.

[50] Chester R, Costa ML, Shepstone L, Cooper A, Donell ST. Eccentric calf muscle training compared with therapeutic ultrasound for chronic Achilles tendon pain-A pilot study. Man Ther 2008; 13:484-91.

[51] Bernathova M, Felfernig M, Rachbauer F, Barthi SD, Martinoli C, Zelger B, Bodner G. Sonographic imaging of abdominal and extraabdominal desmoids. Ultraschall Med 2008; 29:515-9.

[52] Sikdar S, Shah JP, Gilliams E, Gebreab T, Gerber LH. Assessment of Myofascial Trigger Points (MTrPs): A New Application of Ultrasound Imaging and Vibration Sonoelastography. Conf Proc IEEE Eng Med Biol Soc 2008; 5585-8.

[53] Andrade AS, Gaviao MBD, Derossi M, Gameiro GH. Electromyographic activity and thickness of masticatory muscles in children with unilateral posterior crossbite. Clin Anat 2009; 22:200-6.

[54] Hides JA, Stokes MJ, Saide M, Jull GA, Cooper DH. Evidence of lumbar multifidus muscle wasting ipsilateral to symptoms in patients with acute subacute low-back-pain. Spine 1994; 19:165-72.

[55] Ishikawa M, Dousset E, Avela J, Kyrolainen H, Kallio J, Linnamo V, Kuitunen S, Nicol C, Komi PV. Changes in the soleus muscle architecture after exhausting stretch-shortening cycle exercise in humans. Eur J Appl Physiol 2006; 97:298-306.

[56] Hodges PW, Pengel LHM, Herbert RD, Gandevia SC. Measurement of muscle contraction with ultrasound imaging. Muscle Nerve 2003; 27:682-92.

[57] Ferreira PH, Ferreira ML, Hodges PW. Changes in recruitment of the abdominal muscles in people with low back pain - Ultrasound measurement of muscle activity. Spine 2004; 29:2560-6.

[58] Zheng YP, Chan MMF, Shi J, Chen X, Huang QH. Sonomyography: Monitoring morphological changes of forearm muscles in actions with the feasibility for the control of powered prosthesis. Med Eng Phys 2006; 28:405-15.

[59] Guo JY, Zheng YP, Huang QH, Chen X, He JF, Chan H. Performances of one-dimensional sonomyography and surface electromyography in tracking guided patterns of wrist extension. Ultrasound Med Biol 2009; 35: 894-902.

[60] Shi J, Zheng YP, Huang QH, Chen X. Continuous monitoring of sonomyography, electromyography and torque generated by normal upper arm muscles during isometric contraction: Sonomyography assessment for arm muscles. IEEE Trans Biomed Eng 2008; 55:1191-8.

[61] Shi J, Zheng YP, Chen X, Huang QH. Assessment of muscle fatigue using sonomyography: Muscles thickness change detected from ultrasound images. Med Eng Phys 2007; 29: 472-79.

[62] Zhou YJ, Zheng YP. Revoting Hough Transform (RVHT) and its application for muscle fiberorientation estimation in ultrasound images. Ultrasound Med Biol 2008; 34: 1474-81.

[63] Guo JY, Zheng YP, Huang QH, Chen X. Dynamic monitoring of forearm muscles using 1D sonomyography (SMG) system. J Rehab Res Dev 2008; 45:187-96.
[64] Xie HB, Zheng YP, Guo JY, Chen X, and Shi J. Estimation of wrist angle from sonomyography using support vector machine and artificial neural network models. Med Eng Phys 2009; 31: 384-91.
[65] Häkkinen K, Häkkinen A. Muscle cross-sectional area, force production and relaxation characteristics in women at different ages. Eur J Appl Physiol Occup Physiol 1991; 62: 410-4.
[66] Seymour JM, Ward K, Sidhu PS, Puthucheary Z, Steier J, Jolley CJ, Rafferty G, Polkey MI, Moxham J. Ultrasound measurement of rectus femoris crosssectional area and the relationship with quadriceps strength in COPD. Thorax 2009; 64: 418–23.
[67] de Bruin PF, Ueki J, Watson A, Pride NB. Size and strength of the respiratory and quadriceps muscles in patients with chronic asthma. Eur Respir J 1997; 10: 59-64.
[68] Huang QH, Zheng YP, Chen X, Shi J, He JF. Development of a frame-synchronized system for continuous acquisition and analysis of sonomyography, surface EMG and corresponding joint angle. Open Biomed Eng J 2007; 1:77-84.
[69] Bianchi S, Martinoli C. Ultrasound of the Musculoskeletal System. New York: Springer; 2007.
[70] Hakkinen K, Kraemer WJ, Pakarinen A, Triplett-McBride T, McBride JM, Hakkinen A, Alen M, McGuigan MR, Bronks R, Newton RU. Changes in agonist-antagonist EMG, muscle CSA, and force during strength training in middle-aged and older people. J Appl Physiol 1998; 84: 1341-9.
[71] Ploutz-Snyder LL, Convertino VA, Dudley GA. Resistance exercise-induced fluid shifts: change in active muscle size and plasma volume. Am J Physiol 1995; 269: R536-43.
[72] Kawakami Y, Abe T, Kuno SY, Fukunaga T. Training-induced changes in muscle architecture and specific tension. Eur J Appl Physiol O 1995; 72: 37-43.
[73] Kiliaridis S, Kalebo P. Masseter muscle thickness measured by ultrasonography and its relation to facial morphology. J Dent Res 1991; 70: 1262-5.
[74] Lee JP, Wang CL, Shau YW, Wang SF. Measurement of cervical multifidus contraction pattern with ultrasound imaging. J Electromyogr Kinesiol 2009; 19: 391-7.
[75] Jubrias SA, Odderson IR, Esselman PC, Conley KE. Decline in isokinetic force with age: muscle cross-sectional area and specific force. Pflugers Arch 1997; 434:246-53.
[76] Lieber RL. Hypothesis: biarticular muscles transfer moments between joints. Dev Med Child Neurol 1990; 32:456-8.
[77] van Bolhuis BM, Gielen CCAM, van Ingen Schenau GJ. Activation patterns of mono-and bi-articular arm muscles as a function of force and movement direction of the wrist in humans. J Physiol 1998; 508: 313-24.
[78] Jacobs R, Ingen Schenau GJ van. Control of an external force in leg extensions in humans. J Physiol 1992; 457:611-26.
[79] Ebenbichler G, Kollmitzer J, Quittan M, Uhl F, Kirtley C, Fialka V. EMG fatigue patterns accompanying isometric fatiguing knee-extensions are different in mono- and bi-articular muscles. Electroencephalogr Clin Neurophysiol Electromyogr

Mot Contr 1998; 109: 256-62.
[80] Akima H. Kuno S, Takahashi H, Fukunaga T, Katsuta S. The use of magnetic resonance images to investigate the influence of recruitment on the relationship between torque and cross-sectional area in human muscle. Eur J Appl Physiol 2000; 83:475-80.
[81] Henneman E, Somjen, G, Carpenter DD. Functional significance of cell site spinal motoneurons. J Neurophysiol 1965; 28:560-80.
[82] Milner-Brown HS, Stein RB, and Yemm R. The orderly recruitment of human motor units during voluntary isometric contractions. J Physiol 1973; 230: 359-70.
[83] De Luca, CJ, LeFever RS, McCue MP, Xenakisv AP. Behaviour of human motor units in different muscles during linearly varying contractions. J Physiol 1982; 329: 113-28.
[84] Johnson MA, Polgar J, Weightman D and Appleton D. Data on the distribution of fibre types in thirty-six human muscles: An autopsy study. J Neurol Sci 1973; 18:111-29.
[85] Maton B, Petitjean M, Cnockaert JC. Phonomyogram and electromyogram relationships with isometric force reinvestigated in man. Eur J Appl Physiol Occup Physiol 1990; 60: 194-201.
[86] Bilodeau M, Goulet C, Nadeau S, Arsenault AB, Gravel D. Comparison of the EMG power spectrum of the human soleus and gastrocnemius muscles. Eur J Appl Physiol Occup Physiol 1994; 68: 395-401.
[87] Herda TJ, Ryan ED, Beck TW, Costa PB, DeFreitas JM, Stout JR, Cramer JT. Reliability of mechanomyographic amplitude and mean power frequency during isometric step and ramp muscle actions. J Neurosci Methods 2008; 171: 104-9.
[88] Kasai T, Yahagi S. Motor evoked potentials of the first dorsal interosseous muscle in step and ramp index finger abduction. Muscle Nerve 1999; 22: 1419-25.
[89] Torres A, Fiz JA, Galdiz B, Gea J, Morera J, Jane R. A wavelet multiscale based method to separate the high and low frequency components of mechanomyographic signals. Conf Proc IEEE Eng Med Biol Soc 2005; 7262-5.
[90] Farina D, Merletti R, Enoka RM. The extraction of neural strategies from the surface EMG. J Appl Physiol 2004; 96:1486–95.
[91] Herda TJ, Weir JP, Ryan ED, Walter AA, Costa PB, Hoge KM, Beck TW, Stout JR, Cramer JT. Reliability of absolute versus log-transformed regression models for examining the torque related patterns of response for mechanomyographic amplitude. J Neurosci Methods 2009; 179: 240-6.
[92] Orizio C. Muscle sound: bases for the introduction of a mechanomyographic signal in muscle studies. Crit Rev Biomed Eng 1993; 21: 201-43.
[93] Ryan ED, Cramer JT, Housh TJ, Beck TW, Herda TJ, Hartman MJ, Stout JR. Inter-individual variability among the mechanomyographic and electromyographic amplitude and mean power frequency responses during isometric ramp muscle actions. Electromyogr Clin Neurophysiol 2007; 47: 161-73.
[94] Yoshitake Y, Moritani T. The muscle sound properties of different muscle fiber types during voluntary and electrically induced contractions. J Electromyogr Kinesiol 1999;9:209–17.
[95] Akataki K, Mita K,Watakabe M, Itoh K. Mechanomyographic responses during

voluntary ramp contractions of the human first dorsal interosseous muscle. Eur J Appl Physiol 2003; 89:520–5.
[96] Akataki K, Mita K, Watakabe M, Ito K. Age-related change in motor unit activation strategy in force production: a mechanomyographic investigation.Muscle Nerve 2002; 25:505–12.